Phylogeographic structure of the dunes sagebrush lizard, an endemic habitat specialist

Authors

Lauren M. Chan, Department of Biology, Pacific University, Forest Grove, Oregon, USA*

Charles W. Painter, Endangered Species Program, New Mexico Department of Game and Fish, Santa Fe, New Mexico, USA †

Michael T. Hill, Albuquerque, New Mexico, USA.

Toby J. Hibbitts Biodiversity Research and Teaching Collections, Department of Wildlife and Fisheries Sciences, and Natural Resources Institute, Texas A&M University, College Station, Texas, USA

Daniel J. Leavitt, Natural Resources Program, Naval Facilities Engineering Command South West, San Diego, California, USA

Wade A. Ryberg, Natural Resources Institute, Texas A&M University, College Station, Texas, USA

Danielle Walkup, Natural Resources Institute, Texas A&M University, College Station, Texas, USA

Lee A. Fitzgerald, Biodiversity Research and Teaching Collections, Department of Ecology and Conservation Biology, and EEB PhD Program, Texas A&M University, College Station, Texas, USA

* Corresponding author: lchan@pacificu.edu; +1 503-352-1469

† deceased

Keywords: *Sceloporus arenicolus*, fragmentation, conservation genetics, population genetics, shinnery oak sand dunes, Mescalero Sands, Monahans Sandhills.

Short Title: Phylogeography of *Sceloporus arenicolus*

Abstract

Phylogeographic divergence and population genetic diversity within species reflect the impacts of habitat connectivity, demographics, and landscape level processes in both the recent and distant past. Characterizing patterns of differentiation across the geographic range of a species provides insight on the roles of organismal and environmental traits, on evolutionary divergence, and future population persistence. This is particularly true of habitat specialists where habitat availability and resource dependence may result in pronounced genetic structure as well as increased population vulnerability. We use DNA sequence data as well as microsatellite genotypes to estimate range-wide phylogeographic divergence, historical population connectivity, and historical demographics in an endemic habitat specialist, the dunes sagebrush lizard (*Sceloporus arenicolus*). This species is found exclusively in dune blowouts and patches of open sand within the shinnery oak-sand dune ecosystem of southeastern New Mexico and adjacent Texas. We find evidence of phylogeographic structure consistent with breaks and constrictions in suitable habitat at the range-wide scale. In addition, we find support for a dynamic and variable evolutionary history across the range of *S. arenicolus*. Populations in the Monahans Sandhills have deeply divergent lineages consistent with long-term demographic stability. In contrast, populations in the Mescalero Sands are not highly differentiated, though we do find evidence of demographic expansion in some regions and relative demographic stability in others. Phylogeographic history and population genetic differentiation in this species has been shaped by the configuration of habitat patches within a geologically complex and historically dynamic landscape. Our findings identify regions as genetically distinctive

conservation units as well as underscore the genetic and demographic history of different lineages of *S. arenicolus*.

Introduction

Patterns of population genetic diversity within species are shaped by both evolutionary and contemporary history (Rissler, 2016). Though anthropogenic changes to landscapes alter patterns of connectivity that can result in the divergence or coalescence of populations, these processes take place on a background of evolutionary history determined by chance, species' life history, and also geologic and climatic changes. Characterizing this evolutionary history, and identifying the role that organismal traits, evolutionary processes, and ecological conditions have on patterns of phylogeographic divergence adds to our understanding of evolution, and is also fundamental to conserving evolutionary potential in the face of anthropogenic disturbance and climate change (Olivieri et al., 2015).

The phylogeographic history of species can reflect the roles that habitat connectivity, gene flow, and population stability have played in a species' evolutionary persistence. Some species may be characterized by deeply divergent lineages, suggesting a history of limited dispersal and low connectivity among sites (e.g., Richmond et al., 2013, 2014; Chan et al., 2013), especially in ecosystems with steep environmental gradients and discontinuous habitat (Vandergast et al., 2008). Plant and animal taxa in naturally fragmented landscapes, for example, can exhibit strong patterns of genetic population structure with selection favoring limited dispersal. Phylogeographic analyses of *Stenopelmatus* species (Jerusalem crickets) in southwestern North America, for example,

74 revealed limited dispersal among populations, and identified a recent response to
75 anthropogenic change (Vandergast et al., 2007). A meta-analysis of genetic diversity among
76 21 species of terrestrial animals identified hotspots of genetic diversity that may also be
77 regions with high levels of trait divergence due to natural selection (Vandergast et al.,
78 2008). Alternatively, populations may be only weakly divergent across a species' range
79 indicating high connectivity (e.g. Lippé et al., 2006; Chan and Zamudio, 2009) even in the
80 face of strong local dynamics (e.g. Pierson et al., 2013). Identifying evolutionary scenarios
81 and processes that have resulted in particular phylogeographic patterns can help us
82 disentangle processes that underlie population genetic divergence from those that
83 maintain genetic diversity. Understanding the drivers of population genetic structure
84 across the range of a species can also help us predict the response to loss of habitat and the
85 overall vulnerability of species to anthropogenic landscape change.

86 Ecological specialists can have greater population genetic and phylogeographic
87 structure than generalists because individuals and populations may be restricted to
88 spatially isolated patches of suitable habitat. (Roderick et al., 2012; Schär et al., 2018; Wort
89 et al., 2019). Ecological specialists may have narrow physiological tolerances, specific
90 habitat requirements, and be locally abundant but rare at regional scales (Devictor et al.,
91 2008). Habitat specialists use specific landscape features and vegetation associations
92 within their range, and often possess eco-morphological and behavioral adaptations (Miles,
93 1994a, 1994b). Traits that make habitat specialists well-suited for a narrow habitat niche
94 also tend to make them relatively poor dispersers (Clobert et al., 2012). Low tolerance for
95 unsuitable landscapes is expected to restrict movements among isolated patches of
96 preferred habitat. Ecological studies focusing on the demography and distribution of

habitat specialists have found they are sensitive to landscape fragmentation (Leavitt and Fitzgerald, 2013; Walkup et al., 2017).

Local processes are often linked to patterns observed across long-term, evolutionary time scales and at broader spatial scales (see reviews by Cutter, 2013; Rissler, 2016). Thus, in specialists with strict habitat specificity and limited dispersal among populations, we might expect phylogeographic structure to reflect historical patterns of divergence and low population connectivity overall (e.g., Roderick et al., 2012). Alternatively, habitat specialists may have well-connected populations throughout their range, indicating a strong role for dispersal and migration that counters the divergence of potentially isolated local populations across longer time-scales (Pierson et al., 2013). Characterizing evolutionary patterns of divergence and historical demographics in habitat specialists can help us predict the role that short and long-term dynamics play in shaping population genetic structure. In addition, describing spatial patterns of diversity and identifying independent evolutionary units, historical barriers to gene flow, bottlenecks and founder events, and regions of high connectivity allows the effects of contemporary pressures to be disentangled from historical drivers and also provides important information for the future management and conservation of species.

The dunes sagebrush lizard, *Sceloporus arenicolus*, is endemic to the Mescalero and Monahans Sandhills ecosystem of southeastern New Mexico and adjacent Texas (Fitzgerald and Painter, 2009; Laurencio and Fitzgerald, 2010). This species is part of the *Sceloporus graciosus* clade (Chan et al., 2013), but in contrast to other members of this group which tend to be geographically widespread generalists, *S. arenicolus* is a habitat specialist. Within this ecosystem, it only uses shinnery-oak sand dune formations with interconnected

dune blowouts (sandy depressions created by wind) and in some cases shinnery hummocks in dunes with steep slopes (Fitzgerald et al., 1997; Laurencio and Fitzgerald, 2010; Hibbitts et al., 2013). In the Mescalero-Monahans Sandhills Ecosystem, dune blowouts are emergent landforms that are maintained by the interactions among wind, moving sand, and the shinnery oak (*Quercus havardii*) which stabilizes the dunes (Ryberg and Fitzgerald, 2016). Individual *S. arenicolus* lizards demonstrate a nested hierarchy of habitat selection (Fitzgerald et al., 1997), selecting for thermally suitable microhabitats and having preference for relatively large dune blowouts. A sand-diving species, they do not occur in areas with relatively fine sand (Fitzgerald et al. 1997; Ryberg and Fitzgerald 2015). At the highest level of habitat selection, they are endemic to the narrowly distributed Mescalero-Monahans Sandhills (Fitzgerald and Painter, 2009).

Specialists can reach high population densities in their preferred habitat, and can outcompete generalists in the same area even in some degraded habitats (Brown, 1984; Attum et al., 2006). This is true too for *S. arenicolus*, where populations of this ecological specialist thrive where the configuration of key landscape features supports larger groups of interacting individuals, defined as neighborhoods (*sensu* Wright, 1946; Ryberg et al., 2013). Diffusion dispersal throughout interconnected areas of suitable habitat appear key to maintaining populations in contiguous habitat over the long term (Ryberg et al., 2013). The quantity of habitat is positively correlated with the quality of habitat (Smolensky and Fitzgerald, 2011), and the occurrence of *S. arenicolus* is associated with relatively large core areas of shinnery oak dunes.

Since at least the 1930s, anthropogenic disturbances from herbicide spraying, oil and gas mining, and more recently, sand-mining, have resulted in fragmentation and

143 degradation of the shinnery oak dunes. Long-term monitoring and extensive fieldwork also
144 demonstrate that fragmentation of the shinnery oak dunelands leads directly to population
145 collapse because quality of habitat tends to degrade in response to fragmentation, and
146 dispersal is disrupted (Leavitt and Fitzgerald, 2013; Walkup et al., 2017).

147 To adequately inform conservation and management actions, it is necessary to
148 understand the evolutionary history of this species at both broad and fine-scales
149 throughout the range. Previous genetic work confirmed that at broad spatial scales, *S.*
150 *arenicolus* is comprised of at least three distinct genetic groups (Chan et al., 2009).
151 However, it is unclear where these genetic breaks occur geographically and whether they
152 coincide with putative natural or man-made barriers to movement. The purpose of this
153 study is to characterize the evolutionary history of the dunes sagebrush lizard using
154 complete geographic and genetic sampling. To identify evolutionary distinct geographic
155 lineages and to reconstruct the population history of these lineages, we evaluate
156 mitochondrial and nuclear sequence data as well as multilocus microsatellite genotypes.
157 Sampling for individuals occurred evenly throughout the entire known range of this
158 endemic and threatened lizard.

159

160 **Materials and Methods**

161 *Sampling*

162 We surveyed for *Sceloporus arenicolus* throughout their range (Figure 1). Liver or
163 muscle tissue was collected from vouchered specimens deposited in the Biodiversity
164 Research and Teaching Collections (symbolic code: TCWC), or Museum of Southwestern
165 Biology (MSB). Additionally, toe and/or tail tips were collected non-destructively from

166 animals caught in the field that were subsequently released. All tissue samples were stored
167 in 95% EtOH. Whole genomic DNA was extracted from tissues using the DNeasy Blood and
168 Tissue kit (Qiagen).
169
170 *DNA sequence data*
171 We targeted two mitochondrial and four nuclear loci for DNA sequencing. PCR
172 amplification of the mitochondrial loci NADH-dehydrogenase 1 (*ND1*) and cytochrome-b
173 (*cyt-b*) and two protein coding nuclear loci prolactin receptor (*PRLR*) and *R35* used
174 previously published primers (Irwin et al., 1991; Leaché and McGuire, 2006; Leaché, 2010).
175 We used two additional anonymous nuclear loci designed from a genomic library enriched
176 for microsatellite repeats: *sarANL298* (scar298anl.F: 5'-ATGGGAAGGCTTAAAATGAATC;
177 scar298anl.R: 5'-TGTGACTTAGGGAACTGGGTATGT) and *sarANL*875 (scar875anl.F 5'-
178 CTTACCATTCAACCCTTCCTTG; scar875anl.R 5'- CTAGAGCAGACCAGTTCAATGTAAT). All
179 PCR were conducted in 10 µl total volume. Annealing temperature for the new nuclear loci
180 was 54°C.

181 We used 0.4 µl ExoSAP-IT (USB/Affymetrix) and 1.6 µl water to clean 5 µl of PCR
182 product. One µl of clean PCR template was used in each cyclo-sequencing reaction using the
183 same locus-specific primers used in amplification. Sequencing reactions were cleaned and
184 run on an ABI 3730xl at the Duke Sequencing Facility or the Biotechnology Resources
185 Center of Cornell University. Chromatograms were verified and cleaned in Geneious R9
186 (https://www.geneious.com). Heterozygous sites in nuclear sequences were called with
187 the appropriate ambiguity code. Sequences at each locus were aligned using the MAFFT
188 (Katoh, 2005) plug-in in Geneious. All sequence data will be submitted to GenBank.

Because the mitochondrion is inherited as a single unit without recombination, we concatenated the two loci (ND1 and Cyt-*b*) into a single alignment. Each of the four nuclear loci were treated independently. All sequences at each locus were aligned in Geneious and alleles at nuclear loci were determined using the program PHASE (Stephens et al., 2001) and the helper program SeqPHASE (Flot, 2010).

Microsatellite genotype data

Nuclear microsatellite loci were developed from a 454-library enriched for microsatellite motifs developed at Cornell University Evolutionary Genetics Core Facility. After initial screening of loci, we used the Qiagen Type-It microsatellite PCR kit to genotype individuals at these loci in five multiplex reactions (Supp. Mat. Table 1). Forward primers for all loci were tagged with a fluorescent dye and samples were genotyped on an ABI3730xl at the Biotechnology Resource Center of Cornell University with GeneScan 500 LIZ size standard (Thermo Scientific). Alleles were called and verified for all individuals using GeneMarker 2.6. Prior to subsequent genetic analyses, all variable loci were tested for the presence of null alleles and selection by testing for Hardy-Weinberg Equilibrium (HWE) and for evidence of linkage disequilibrium using GenePop (Rousset, 2007). The final dataset included genotypes for all individuals at 27 variable and neutrally evolving nuclear microsatellite loci.

Data analysis

Summary statistics

We used PAUP (Swofford, 2002) to determine the number of parsimony informative sites for each sequence alignment and DNAsp v6 (Rozas et al., 2017) to calculate the number of unique haplotypes, the number of segregating sites (S), nucleotide diversity (π), and the average number of nucleotide differences (k) for each sequence alignment.

Haplotype networks

We constructed parsimony networks in TCS (Clement et al., 2000) for complete mtDNA haplotypes for *S. arenicolus.* Because the results generated by network methods can be strongly influenced by missing data (Joly et al., 2007), we first omitted all individuals with missing sequence data for one of the two mitochondrial loci. We additionally omitted individuals for which we did not have locality information. The final haplotype network for mtDNA contained 195 individuals. We additionally constructed parsimony networks for the phased alleles at each nuclear locus.

Phylogenetic analysis

For the mitochondrial DNA, we estimated the phylogenetic relationships among *S. arenicolus* under both maximum likelihood and Bayesian frameworks. *Urosaurus ornatus*, *Uta stansburiana*, *Phrynosoma coronatum*, *Sceloporus jarrovii*, *S. merriami*, *S. occidentalis*, and nine individuals of *S. graciosus* were used as outgroups (following Chan et al., 2013). Concatenated mtDNA alignments were first reduced to unique sequences using a Python script from BioPython (sequence_cleaner.py). We estimated the best-fit model of sequence evolution at each codon position of each gene in DT-ModSel (Minin et al., 2003) and partitioned phylogenetic analyses by gene and codon position. The best fit models by DT-

ModSel were a SYM+G for the first codon position of each gene, HKY+I for the second codon position of each gene, and TrN + I + G and TrN + G for the third codon position of *ND1* and *Cyt-b* respectively. We estimated the phylogeny under a Bayesian framework in MrBayes v3.2.6 (Ronquist and Huelsenbeck, 2003; Ronquist et al., 2012) excluding individuals with missing data. TrN models were expanded to GTR for Bayesian analyses and the final analysis consisted of two independent runs each of 50 million generations sampled every 5,000 generations. All parameters were checked for adequate mixing and convergence, and the maximum clade credibility tree was summarized in MrBayes.

Population genetic analysis

We estimated within population diversity and among population pairwise F_{ST} for mtDNA as well as microsatellite data assuming membership to the phylogroups based on the Bayesian phylogeny. Estimates of F_{ST} were done in Arlequin (Excoffier and Lischer, 2010) for mtDNA and in FSTAT for microsatellite data. Because samples were distributed evenly throughout the range of *S. arenicolus*, we additionally conducted population genetic analyses without any assumption of population membership using assignment methods in Structure 2.3.4 (Pritchard et al., 2000). In Structure, we tested assignment of all individuals to *K* populations from K=1 to 10. At each K we conducted 10 replicate runs each consisting of 1 million generations with the first 50% discarded as burn-in. We used StructureHarvester (Earl and vonHoldt, 2011) to examine all runs and CLUMPP (Jakobsson and Rosenberg, 2007) and DISTRUCT (Rosenberg, 2004) to visualize population membership. Structure runs with all individuals supported K=2, so subsequent runs investigated further partitioning with each major group. For each subset of data, we tested

K=1 to 5 each with 10 replicate runs at each K each consisting of 2 million runs with the first 50% discarded as burn-in.

Demographic analyses

We estimated the historical demographics for each of five primary phylogeographic regions (A-E) identified in mtDNA analyses. We used multilocus sequence data to construct extended Bayesian skyline plots in BEAST 2.5.0 (Drummond et al., 2005, 2012; Heled and Drummond, 2008). Each dataset included concatenated mtDNA alignments in addition to phased genotypes for each of the four nuclear loci. Substitution models for each locus were set based on MrModeltest (Nylander, 2004; Supp. Mat. Table 2). All runs assumed a relaxed molecular clock with a log-normal distribution for the mtDNA partition and strict molecular clocks for the nuclear partitions. The rate for mtDNA was set with a log normal distribution with mean of $1x10^{-8}$ substitutions/site/year and SD of 0.27 following (Chan et al., 2013). Parameter trends were examined in Tracer to check for adequate mixing within runs and convergence across runs. Final runs were 50 million steps sampled every 5,000 steps for regions B, C, and E. The final runs for regions A and D were 100 and 200 million steps sampled every 10,000 and 20,000 steps, respectively. Extended Bayesian skyline plots we generated after discarding the first 25% sampled steps as burn-in.

Hypothesis testing

Based on the results of phylogenetic analyses and assignment tests, we tested three alternative hypotheses of divergence and population expansion among three geographic groups (Northern Mescalero Sands, Southern Mescalero Sands, and Monahans Sandhills)

assuming that the Monahans Sandhills populations were ancestral and of constant population size (Chan et al., 2009; Supp. Mat. Figure 1). We used approximate Bayesian computation to evaluate support for these models and estimate demographic parameters of the best supported model in DIYABC (Cornuet et al., 2008). Analyses included mtDNA and phased nuclear sequences. Locus parameters were specified after estimation of substitution models for each locus in DT-ModSel. The prior for the mtDNA mutation rate was set as a normal distribution with a mean of $1x10^{-8}$ substitutions per site per year and nuclear substitution rates were set as uniform distributions. Initial runs were used to determine adequate priors for demographic parameters. The final analysis included 2 million samples for each divergence model (6 million total) with a linear regression step to extract the closest 1% of samples and determine the best supported model of the three. For the best supported model, we used the same selection/rejection process to estimate divergence times and demographic parameters from the closest 1% of the 2 million samples.

Results

Summary statistics

Sample sizes, alignment lengths, the number of unique haplotypes, number of segregating sites, average nucleotide differences, and nucleotide diversity are reported in Supp. Mat. Table 3. As expected, nuclear loci were less variable than mtDNA though nucleotide diversity was similar for mtDNA and two nuclear loci. We also recovered multilocus genotypes for 237 individuals at 27 microsatellite loci that conformed to HWE

302 expectations and did not show any evidence of linkage or null alleles. The average number
303 of alleles per locus was 16.4 with a range from 3 to 35 (Supp. Mat. Table 4).
304
305 *Haplotype networks and phylogenetics*
306 Mitochondrial haplotype networks revealed geographically associated haplotype
307 groups for mtDNA that largely correspond to regions of grossly contiguous habitat (Figure
308 2). In the Northern Mescalero Sands, there are three main haplotype groups corresponding
309 largely with the A regions (Figure 1; AA and AB), the B regions (BA and BB), and the C
310 region, though the genetic divergence among these three groups is small. Common
311 haplotypes are shared across regions, but derived haplotypes are unique to each region.
312 Regions AB and BB have genetic diversity that is primarily a subset of the diversity found in
313 AA and BA, respectively. The Southern Mescalero Sands (Regions DA and DB) are
314 genetically divergent from the Northern Mescalero Sands populations with the barrier
315 between the two groups reflecting a west-east constriction in the distribution of potentially
316 suitable habitat (referred hereafter as "the Skinny Zone"). Among the Southern Mescalero
317 Sands individuals in region DA, we find a single widespread haplotype and multiple derived
318 haplotypes. In addition, region DB at southernmost tip of the Southern Mescalero Sands
319 contains a cluster of derived haplotypes.
320 Populations in the Monahans Sandhills are genetically distinct from all other *S.*
321 *arenicolus* populations, but do not form a single haplotype group. There is high sequence
322 divergence among haplotypes from the Monahans Sandhills despite occurring in a
323 relatively restricted geographic area and they are distantly related to Mescalero Sands
324 haplotypes. The EA and EC areas each have unique haplotypes without a single, most

common haplotype. The EB haplotypes fall out into two main groups, one that is equally distant to northern and southern Mescalero Sands haplotypes and one that is distantly related to all other recovered haplotypes (Figure 2).

In general, nuclear gene regions had much lower genetic diversity with very little genetic structure (Supp. Mat. Figure 2). Across all four nuclear loci, we found a similar pattern with the most common haplotypes occurring in most, or all regions. At PRLR and scar875, several derived loci were unique to Monahans Sandhills populations and Monahans Sandhills plus Southern Mescalero Sands populations. With one exception (AB locus R35) regions AA, AB, and BB did not have any unique nuclear alleles.

Phylogenetic reconstructions largely corroborated the groups found in the network analyses (Figure 3). We recover *S. arenicolus* as monophyletic (PP = 1). Monahans Sandhills populations were paraphyletic with respect to Mescalero Sands populations with the southern-most Monahans Sandhills individuals forming a weakly supported clade (PP = 0.8657) sister to all other *S. arenicolus*. Among the remaining individuals, there is strong support for a Northern Mescalero Sands clade including individuals north of the skinny zone (PP = 0.9758) and moderate support for a Southern Mescalero Sands – Monahans Sandhills clade that includes individuals south of the skinny zone and the northern and central Monahans Sandhills (PP = 0.9345). Within the Northern Mescalero Sands clade, we recover support for some clusters of individuals, but do not find well-supported clades corresponding to distinct geographic regions. Individuals from region A, at the northern end of the range, form a basal polytomy relative to otherwise well-supported clades containing most individuals from regions B and C, and several from region A and one from D (TCWC 94831). Support for a clade that includes most B individuals is high (PP = 0.9639)

as is support for two different clades that each primarily include individuals from C (PP = 1). We do not recover very much genetic resolution for individuals south of the skinny zone in the Southern Mescalero Sands or the northern or central Monahans Sandhills. Notably, individuals from Monahans Sandhills are paraphyletic and their relationships largely unresolved. While most individuals from regions cluster with other individuals from the same region, as expected from the haplotype network, there are a few individuals that fall out with individuals from different regions.

Demographic estimates

Extended Bayesian skyline plots match the inferences made from the haplotype networks (Supp. Mat. Figure 3). We see evidence of recent population expansion in region D and demographic stability in region E. Regions A, B, and C show some evidence of population expansion though the credible intervals around the most recent population sizes is large and does not exclude the possibility of demographic stability.

Population Genetics

Pairwise F_{ST} among populations was high among regions with values significantly different from zero ranging from 0.099 to 0.904 for mtDNA and 0.026 to 0.236 based on microsatellite loci (Table 1).

Assignment tests based on microsatellite data reveal nested structure at multiple spatial scales (Figure 4). Across all samples, our analyses recover two groups with some admixture. The geographic break between these two groups corresponded to the Skinny Zone of the Mescalero Sands with some individuals in this area being admixed. Further

371 assignment tests in Structure with nested subsets of the data indicate that these admixed
372 individuals are aligned with individuals in the Southern Mescalero Sands. We recover
373 distinctive groups in the Northern Mescalero Sands with some admixture as well. Region A
374 individuals are distinct from region B + C individuals although, assignment plots suggest
375 some admixture between western A populations (AA) and populations in region C,
376 corroborating results from the mtDNA haplotype networks. Analysis of the AA-AB groups
377 recover AB as genetically distinct corroborating F_{ST} estimates (Table 1). Analysis of the BA-
378 BB-C group supports BB and C as distinct from one another with BA having genetic
379 affinities to both. Together these results show a clear genetic break between the Southern
380 Mescalero Sands and Monahans Sandhills populations. For the Southern Mescalero Sands
381 populations there is an additional genetic break between regions DA and DB coinciding
382 with another constriction in suitable habitat. Among Monahans Sandhills samples, EA
383 individuals are largely distinct from EB+EC. Individuals from EB and EC are somewhat
384 distinct from one another though not all individuals within a region cluster unambiguously
385 with others in the group.
386
387 *Hypothesis testing*
388 We recover strongest support (PP = 0.9991) for a divergence scenario that involved
389 colonization of the Northern Mescalero Sands from Monahans Sandhills populations
390 around 34.8 Kya (CI 17.7-108 Kya) followed by colonization of the Southern Mescalero
391 Sands from Monahans Sandhills populations more recently, around 16.3 Kya (CI 7.9-41
392 Kya; Figure 5). It is possible that the initial colonization of Northern Mescalero Sands
393 included colonization of the Southern Mescalero Sands, with subsequent local extinction

and recolonization, or genetic replacement. It is important to note that the 95% credible intervals for all estimates of divergence time and population size are broad. In fact, though the time of expansion in the Northern Mescalero Sands (T_{exp1})was constrained in individual ABC simulations to occur after the divergence between the Northern Mescalero Sands and the other regions (T_{anc}), the median estimate for the former T_{exp1} precedes the median divergence time, T_{anc} (Figure 5), though both estimates have extremely broad and overlapping credible intervals.

Discussion

Sampling of *S. arenicolus* throughout the entire range provides greater resolution of the evolutionary patterns of divergence of this narrowly distributed habitat specialist. We find support for multiple genetic groups within *S. arenicolus* suggesting limited migration in this habitat specialist. In particular, we find genetic structure beyond the three mitochondrial groups described in Chan et al. (2009). Patterns of divergence recovered by mtDNA corroborate nuclear microsatellite data and demonstrate the importance of the landscape-scale configuration of areas of habitat on the phylogeographic structure of this habitat specialist. With thorough geographic sampling we are able to identify regions that have served as barriers to population connectivity and characterize historical demographics across evolutionary time scales.

Lineages of *S. arenicolus* in the Mescalero Sands and Monahans Sandhills have independent and distinct histories that are associated with the timing of sand deposition and dune formation in these sub-regions. Indeed, the Mescalero Sands and Monahans Sandhills have related, but distinguishable geologic histories (Muhs and Holliday, 2001;

Rich and Stokes, 2011; Muhs, 2017). Both Mescalero Sands and Monahans Sandhills are sand sheets of the Southern High Plains deposited over older, compact eolian deposits comprising the Black Water Draw formation (204 - 43 Kya; Rich and Stokes, 2011). Sand accumulation and dune formation has occurred repeatedly with current sand sheet age estimates for Mescalero and Monahans as 29.2 and 22.2 Kya respectively and with a more recent deposition ~ 7.5 Kya (Rich and Stokes, 2011). Though *S. arenicolus* sampled from the Monahans Sandhills do not form a monophyletic group, it is clear that they are distinct from Mescalero Sands populations with estimated initial divergence between these two regions occurring long ago (34.8 Kya, CI 108-17.7 Kya; Figure 5). While the estimated divergence is older than the estimated age of the most recent sand deposition, this is a dynamic landscape that has undergone cycles of sand deposition during periods of aridity (Holliday, 1989; Rich and Stokes, 2011) such that this divergence is most likely associated with previous episodes of sedimentation and dune formation. There are broad CI around estimates of divergence and population expansion, but these estimates generally coincide with the sand age of Northern Mescalero Sands. Furthermore, the estimate of the most recent deposition falls within the CI for colonization and expansion times for the Southern Mescalero Sands.

The location and movement of sand dune formations has changed over millennia (Muhs and Holliday, 1995, 2001; Muhs, 2017). While the presence of sand dunes alone does not indicate the presence of shinnery oak-sand dune ecosystem, the distribution of habitat suitable to *S. arenicolus* has likely shifted in its occurrence and connectivity over geologic time. Given the dynamic nature of the landscape to which *S. arenicolus* is endemic, it stands to reason that dynamic histories also characterize the phylogeographic and population

genetic structure in this species. Though the age of the Mescalero Sands and Monahans Sandhills geologic formations are uncertain, our data suggest that Monahans Sandhills was the source population from which Mescalero Sands *S. arenicolus* populations were colonized. Mescalero Sands populations, which lie to the north of the Monahans Sandhills, are comprised of at least two distinct lineages, but nuclear microsatellite data and ABC analyses suggest that the Southern Mescalero Sands populations are more closely related to the Monahans Sandhills populations than to northern Mescalero Sands populations. The two sand formations are not currently connected by suitable habitat (Figure 1), but presumably were connected in the past facilitating the colonization of Mescalero Sands from Monahans Sandhills. by *S. arenicolus*. The current range map (Figure 1) is informed by currently occupied habitat, but given the dynamic history of the shinnery oak-sand dune ecosystem, potentially suitable habitat connecting regions may have occurred in the past. The configuration of available habitat is varies across time which presumably causes concordant shifts in species' distributions.

Our genetic data suggest that the colonization event associated with the current Southern Mescalero Sands populations occurred separately from the event that resulted in the Northern Mescalero Sands populations. Colonization of the Northern Mescalero Sands and divergence from the Monahans Sandhill source population is estimated to have occurred approximately 34 Kya followed by population expansion (Figure 5; Supp. Mat. Figure 3). While recognizing that there are broad confidence intervals around the estimated time of this event, it is plausible that this divergence was associated with the deposition of loose aeolian sands over the Blackwater Draw Formation (Rich and Stokes, 2011). The second divergence was between the southern Mescalero Sands and Monahans

463 Sandhills occurring later, around 16.3 Kya. This is similar to the age of more recent sand
464 deposits in the Mescalero Sands, and subsequent population expansion with a median
465 estimate of 9.9 Kya coincides roughly with the ages of the most recent aeolian deposits.
466 This result suggests that after the colonization of the Mescalero Sands 34 Kya by *S.*
467 *arenicolus,* habitat between the Mescalero Sands and Monahans Sandhills contracted or
468 that Southern Mescalero Sands populations became extirpated and this area was later
469 recolonized. Both scenarios seem plausible given what we know about *S. arenicolus* ecology
470 and the dynamic nature of this system.

471 *Sceloporus arenicolus* requires interconnected shinnery-oak blowouts to support
472 populations (Ryberg et al., 2013; Leavitt and Fitzgerald, 2013). Shinnery oak flats or
473 isolated dune blowouts impede movements and isolate populations. The divergences that
474 we see across the Mescalero Sands and Monahans Sandhills correspond largely with the
475 geographic extent of potentially suitable habitat identified in several studies of *S. arenicolus*
476 (Fitzgerald et al., 1997; Laurencio and Fitzgerald, 2010; Walkup et al., 2018). We are also
477 able to reconstruct historical population demography and recover variable, and sometimes
478 dynamic, histories across populations of *S. arenicolus*. For instance, we find support for a
479 major genetic break that coincides with the Skinny Zone, a narrow constriction (~ 3 km
480 wide) in the central Mescalero Sands. This narrow zone of habitat for *S. arenicolus* is
481 indicative of a long-standing barrier to dispersal and is now a point of secondary contact
482 between divergent Northern and Southern Mescalero Sands populations.

483 We find shallow divergence, but distinct genetic diversity among the Northern
484 Mescalero Sands regions indicating that habitat suitability also impacts population genetic
485 connectivity at these finer spatial scales. Populations in some of these regions, like AB and

BB, have diverged in isolation, suggesting a founder effect in line with the major direction of sand dune movement (Muhs, 2017). We additionally confirm a recent colonization and subsequent rapid population expansion in the southern portion of the Mescalero Sands (Region D). Finally, among the Monahans Sandhills samples we documented highly divergent alleles, deep divergence among populations, and relative population stability. We recovered at least three divergent groups among the Monahans Sandhills individuals indicating limited movement among older populations retaining ancestral genetic diversity.

The historical demography and patterns of divergence are reflected in the microsatellite data as well as the more slowly evolving mtDNA sequence data indicating that population structure is the result of longstanding habitat dynamics and restrictions to gene flow at multiple spatial scales, not just more recent anthropogenic change. Demographic studies of *S. arenicolus* have emphasized the importance of a network of suitable habitat at multiple spatial scales to support metapopulation dynamics and population persistence (Ryberg et al., 2014). Landscape-ecological analyses of presence and absence of lizard community membership across the Mescalero Sands demonstrated that landscape heterogeneity, not dispersal, explained community assembly and meta-community structure (Ryberg and Fitzgerald, 2015, 2016). The occurrence of the habitat specialist *S. arenicolus* was a driver of this pattern. As such, because the fine-scale distribution of suitable habitat is critical for local presence of *S. arenicolus*, we suggest the composition and configuration of the landscape with respect to unsuitable habitat types determines patterns of genetic connectivity across the range. The divergences we detect reinforce that extensive habitat may be necessary to support gene flow among populations and that habitat quality and habitat configuration at finer scales may be of critical

importance to identifying potential corridors. Importantly, it is clear that the shinnery oak-sand dune ecosystem is a dynamic landscape where the configuration of habitat patches can change over decades and millennia. We know from phylogeographic studies that specialists in changing environments undergo repeated episodes of isolation and divergence (Roderick et al., 2012). While it is impossible to reconstruct the specific, chronological habitat configuration for the Mescalero Sands and Monahans Sandhills, it is likely that networks of suitable habitat have diverged and coalesced repeatedly over time (e.g., Dzialak et al., 2013). Source-sink dynamics are important at local and contemporary spatial and temporal scales (Ryberg et al., 2013; Walkup et al., 2019), and this may translate to evolutionary patterns of population genetic structure at broader spatial scales and longer time scales. Under this model, habitat patches shift in their extent and distribution over time due to geological processes. The divergence and coalescence of habitat patches across time results in repeated local extinction, population divergence, and recolonization. In support of this scenario, we find population genetic and demographic patterns that reflect such dynamic processes and their variability across the landscape. For instance, the Southern Mescalero Sands is a more rapidly shifting sand dune formation (Muhs and Holliday, 1995, 2001; Muhs, 2017) in comparison to the sand sheets of the Monahans Sandhills formation which are more stable and less dynamic (Machenberg, 1984). The Southern Mescalero Sands may be characterized by local extinction and recolonization whereas the slower movement of the Monahans Sandhills may maintain demographically stable and isolated populations over longer time periods.

The patterns of divergence and gene flow that we see in *S. arenicolus* are not surprising of a habitat specialist inhabiting a dynamic landscape. Based on demographic

studies (Leavitt and Fitzgerald, 2013; Walkup et al., 2019) and observations of *S. arenicolus* (Ryberg et al., 2012; Leavitt and Acre, 2014; Walkup et al., 2018, p. 2018; Young et al., 2018), individuals do not move large distances. Their strict habitat requirements, and the naturally patchy and temporally dynamic qualities of this habitat, suggests that populations should be subdivided. The nestedness of genetic structure in *S. arenicolus* mirrors the hierarchical nature of their habitat preference: individuals require suitable blowouts within a matrix of shinnery oak, and populations are supported by a network of connected shinnery oak-sand dune complexes. While the genetic consequences of metapopulation dynamics have typically been explored at fine spatial and temporal scales, our phylogeographic study shows that these metapopulation dynamics may also leave their signature at broader spatial scales, in this case, across the range of this endemic lizard.

Conservation

The shinnery oak-sand dune habitats of Mescalero Sands and Monahans Sandhills have experienced severe habitat degradation and fragmentation, particularly in the southern portions of the range of *S. arenicolus* (Leavitt and Fitzgerald, 2013; Walkup et al., 2017). Recent ongoing fragmentation due to human activities (e.g. highways and caliche roads built for oil field development) is known to decrease connectivity among populations and interrupt metapopulation dynamics leading to extinction of local populations (Ryberg et al., 2013, 2014; Leavitt and Fitzgerald, 2013; Walkup et al., 2017). Fragmentation of the shinnery oak-sand dune ecosystem increases the likelihood that ancestral diversity and unique evolutionary lineages will be lost. Our findings highlight regions to be considered as

554 genetically distinctive conservation units as well as underscore the unique genetic and
555 demographic history of different regions within the range of *S. arenicolus*.

556

557 **Acknowledgments**

558 Thank you to J. T. Giermakowski (MSB), R. Macey, C. Spencer (MVZ), and J. Vindum (CAS)
559 for access to tissue samples. We thank the many research assistants who helped with tissue
560 collection, DNA sequencing, and genotyping, including J. Moberg, E. Gibson, D. Cavero, and
561 T. Caspi. Sequencing was conducted at the Genome Sequencing & Analysis Core Resource of
562 the Duke Institute for Genome Sciences and Policy. Genotyping of microsatellite loci was
563 completed at the Biotechnology Core Facility of Cornell University. Portions of this
564 research were provided by the Dunes Sagebrush Lizard/ Lesser Prairie Chicken Candidate
565 Conservation Agreement (CCA) Research Fund administered by CEHMM, Carlsbad, New
566 Mexico, and by USA Bureau of Land Management, and by the State of Texas Comptroller of
567 Public Accounts. This is contribution number xxxx of the Biodiversity Research and
568 Teaching Collections, Texas A&M University.

569

570 **Literature Cited**

571 Attum, O., Eason, P., Cobbs, G., and Baha El Din, S.M. 2006. Response of a desert lizard
572 community to habitat degradation: Do ideas about habitat specialists/generalists
573 hold? *Biological Conservation* 133: 52–62.
574 Brown, J.H. 1984. On the relationship between abundance and distribution of species.
575 *American Naturalist* 124: 255–279.
576 Chan, L.M., Archie, J.W., Yoder, A.D., and Fitzgerald, L.A. 2013. Review of the systematic
577 status of *Sceloporus arenicolus* Degenhardt and Jones, 1972 with an estimate of
578 divergence time. *Zootaxa* 3664: 312–320.
579 Chan, L.M., Fitzgerald, L.A., and Zamudio, K.R. 2009. The scale of genetic differentiation in
580 the Dunes Sagebrush-Lizard (*Sceloporus arenicolus*), an endemic habitat specialist.
581 *Conservation Genetics* 10: 131–142.

582 Chan, L.M., and Zamudio, K.R. 2009. Population differentiation of temperate amphibians in
583 unpredictable environments. *Molecular Ecology* 18: 3185–3200.
584 Clement, M., Posada, D., and Crandall, K.A. 2000. TCS: a computer program to estimate gene
585 genealogies. *Molecular Ecology* 9: 1657–1659.
586 Clobert, J., Baguette, M., Benton, T.G., and Bullock, J.M. 2012. Dispersal Ecology and
587 Evolution. Oxford University Press, Oxford, UK.
588 Cornuet, J.M., Santos, F., Beaumont, M.A., Robert, C.P., Marin, J.M., Balding, D.J., Guillemaud,
589 T., and Estoup, A. 2008. Inferring population history with DIY ABC: a user-friendly
590 approach to approximate Bayesian computation. 24: 2713–2719.
591 Cutter, A.D. 2013. Integrating phylogenetics, phylogeography and population genetics
592 through genomes and evolutionary theory. *Molecular Phylogenetics and Evolution*
593 69: 1172–1185.
594 Devictor, V., Julliard, R., and Jiguet, F. 2008. Distribution of specialist and generalist species
595 along spatial gradients of habitat disturbance and fragmentation. *Oikos* 117: 507–
596 514.
597 Drummond, A.J., Rambaut, A., Shapiro, B., and Pybus, O.G. 2005. Bayesian coalescent
598 inference of past population dynamics from molecular sequences. 22: 1185–1192.
599 Drummond, A.J., Suchard, M.A., Xie, D., and Rambaut, A. 2012. Bayesian phylogenetics with
600 BEAUti and the BEAST 1.7. 29: 1969–1973.
601 Dzialak, M.R., Houchen, D.J., Harju, S.M., and Mudd, J.P. 2013. Ecosystem-level dynamics of
602 soil-vegetation features, with implications for conserving a narrowly endemic
603 reptile. *Landscape Ecology* 28: 1371–1385.
604 Earl, D.A., and vonHoldt, B.M. 2011. STRUCTURE HARVESTER: a website and program for
605 visualizing STRUCTURE output and implementing the Evanno method. *Conservation*
606 *Genetics Resources* 4: 359–361.
607 Excoffier, L., and Lischer, H.E.L. 2010. Arlequin suite ver 3.5: a new series of programs to
608 perform population genetics analyses under Linux and Windows. *Molecular Ecology*
609 *Resources* 10: 564–567.
610 Fitzgerald, L., Painter, C., Sias, D., and Snell, H. 1997. The range, distribution, and habitat of
611 *Sceloporus arenicolus* in New Mexico: final report submitted to the New Mexico
612 Department of Game and Fish (Contract #80-516.6-01).
613 Fitzgerald, L.A., and Painter, C.W. 2009. Dunes Sagebrush Lizard (*Sceloporus arenicolus*). *In*
614 Lizards of the American Southwest: A Photographic Field Guide. *Edited by* L.L.C.
615 Jones and R.E. Lovich. Rio Nuevo Publishers, Tucson, Arizona. pp. 198–120.
616 Flot, J.-F. 2010. SeqPHASE: a web tool for interconverting phase input/output files and fasta
617 sequence alignments. *Molecular Ecology Resources* 10: 162–166.
618 Heled, J., and Drummond, A. 2008. Bayesian inference of population size history from
619 multiple loci. *BMC Evolutionary Biology* 8: 289.
620 Hibbitts, T.J., Ryberg, W.A., Adams, C.S., Fields, A.M., Lay, D., and Young, M.E. 2013.
621 Microhabitat selection by a habitat specialist and a generalist in both fragmented
622 and unfragmented landscapes. *Herpetological Conservation and Biology* 8: 104–113.
623 Holliday, V.T. 1989. The Blackwater Draw Formation (Quaternary): a 1.4-plus-m.y. record
624 of eolian sedimentation and soil formation on the Southern High Plains. *Geological*
625 *Society of America Bulletin* 101: 1598–1607.
626 Irwin, D.M., Kocher, T.D., and Wilson, A.C. 1991. Evolution of the cytochrome b gene of
627 mammals. *Journal Of Molecular Evolution* 32: 128–144.

628 Jakobsson, M., and Rosenberg, N.A. 2007. CLUMPP: a cluster matching and permutation
629 program for dealing with label switching and multimodality in analysis of
630 population structure.
631 Joly, S., Stevens, M.I., and van Vuuren, B.J. 2007. Haplotype networks can be misleading in
632 the presence of missing data. *Systematic Biology* 56: 857–862.
633 Katoh, K. 2005. MAFFT version 5: improvement in accuracy of multiple sequence
634 alignment. *Nucleic Acids Research* 33: 511–518.
635 Laurencio, L.R., and Fitzgerald, L.A. 2010. Atlas of distribution and habitat of the dunes
636 sagebrush lizard (*Sceloporus arenicolus*) in New Mexico. *Texas Cooperative Wildlife*
637 *Collection*.
638 Leaché, A.D. 2010. Species trees for spiny lizards (Genus *Sceloporus*): Identifying points of
639 concordance and conflict between nuclear and mitochondrial data. 54: 162–171.
640 Leaché, A.D., and McGuire, J. 2006. Phylogenetic relationships of horned lizards
641 (*Phrynosoma*) based on nuclear and mitochondrial data: Evidence for a misleading
642 mitochondrial gene tree. 39: 628–644.
643 Leavitt, D.J., and Acre, M.R. 2014. *Sceloporus arenicolus*, activity patterns and foraging
644 mode. *Herpetological Review* 45: 699–700.
645 Leavitt, D.J., and Fitzgerald, L.A. 2013. Disassembly of a dune-dwelling lizard community
646 due to landscape fragmentation. *Ecosphere* 4: art97.
647 Lippé, C., Dumont, P., and Bernatchez, L. 2006. High genetic diversity and no inbreeding in
648 the endangered copper redhorse, *Moxostoma hubbsi* (Catostomidae, Pisces): the
649 positive sides of a long generation time. *Molecular Ecology* 15: 1769–1780.
650 Machenberg, M.D. 1984. Geology of Monahans Sandhills State Park, Texas. : 49.
651 Miles, D.B. 1994a. Population differentiation in locomotor performance and the potential
652 response of a terrestrial organism to global environmental change. *American*
653 *Zoologist* 34: 422–436.
654 Miles, D.B. 1994b. Covariation between morphology and locomotory performance in
655 sceloporine lizards. *In* Lizard Ecology: Historical and Experimental Perspectives.
656 *Edited by* L.J. Vitt and E.R. Pianka. Princeton University Press. pp. 207–235.
657 Minin, V., Abdo, Z., Joyce, P., and Sullivan, J. 2003. Performance-based selection of likelihood
658 models for phylogeny estimation. *Systematic Biology* 52: 674–683.
659 Muhs, D.R. 2017. Evaluation of simple geochemical indicators of aeolian sand provenance:
660 Late Quaternary dune fields of North America revisited. *Quaternary Science Reviews*
661 171: 260–296.
662 Muhs, D.R., and Holliday, V.T. 1995. Evidence of active dune sand on the Great Plains in the
663 19th century from accounts of early explorers. *Quaternary Research* 43: 198–208.
664 Muhs, D.R., and Holliday, V.T. 2001. Origin of late Quaternary dune fields on the Southern
665 High Plains of Texas and New Mexico. *Geological Society of America Bulletin*: 13.
666 Nylander, J. 2004. MrModeltest v2. Program distributed by the author.
667 Olivieri, I., Tonnabel, J., Ronce, O., and Mignot, A. 2015. Why evolution matters for species
668 conservation: perspectives from three case studies of plant metapopulations.
669 *Evolutionary Applications* 9: 196–211.
670 Pierson, J.C., Allendorf, F.W., Drapeau, P., and Schwartz, M.K. 2013. Breed locally, disperse
671 globally: fine-scale genetic structure despite landscape-scale panmixia in a Ffire-
672 specialist. *PLoS ONE* 8: e67248.

673 Pritchard, J., Stephens, M., and Donnelly, P. 2000. Inference of population structure using
674 multilocus genotype data. *Genetics* 155: 945–959.
675 Rich, J., and Stokes, S. 2011. A 200,000-year record of late Quaternary Aeolian
676 sedimentation on the Southern High Plains and nearby Pecos River Valley, USA.
677 *Aeolian Research* 2: 221–240.
678 Richmond, J.Q., Backlin, A.R., Tatarian, P.J., Solvesky, B.G., and Fisher, R.N. 2014. Population
679 declines lead to replicate patterns of internal range structure at the tips of the
680 distribution of the California red-legged frog (*Rana draytonii*). *Biological*
681 *Conservation* 172: 128–137.
682 Richmond, J.Q., Barr, K.R., Backlin, A.R., Vandergast, A.G., and Fisher, R.N. 2013.
683 Evolutionary dynamics of a rapidly receding southern range boundary in the
684 threatened California Red-Legged Frog (*Rana draytonii*). *Evolutionary Applications*
685 6: 808–822.
686 Rissler, L.J. 2016. Union of phylogeography and landscape genetics. *PNAS* 113: 8079–8086.
687 Roderick, G.K., Croucher, P.J.P., Vandergast, A.G., and Gillespie, R.G. 2012. Species
688 Differentiation on a Dynamic Landscape: Shifts in Metapopulation Genetic Structure
689 Using the Chronology of the Hawaiian Archipelago. *Evol Biol* 39: 192–206.
690 Ronquist, F., and Huelsenbeck, J. 2003. MrBayes 3: Bayesian phylogenetic inference under
691 mixed models. 19: 1572–1574.
692 Ronquist, F., Teslenko, M., van der Mark, P., Ayres, D.L., Darling, A., Höhna, S., Larget, B., Liu,
693 L., Suchard, M.A., and Huelsenbeck, J.P. 2012. MrBayes 3.2: efficient Bayesian
694 phylogenetic inference and model choice across a large model space. *Systematic*
695 *Biology* 61: 539–542.
696 Rosenberg, N. 2004. DISTRUCT: a program for the graphical display of population
697 structure. *Molecular Ecology Notes* 4: 137–138.
698 Rousset, F. 2007. Genepop'007: a complete re-implementation of the Genepop software for
699 Windows and Linux. *Molecular Ecology Notes* 8: 103–106.
700 Rozas, J., Ferrer-Mata, A., Sánchez-DelBarrio, J.C., Guirao-Rico, S., Librado, P., Ramos-Onsins,
701 S.E., and Sánchez-Gracia, A. 2017. DnaSP 6: DNA Sequence Polymorphism Analysis
702 of Large Data Sets. *Molecular Biology and Evolution* 34: 3299–3302.
703 Ryberg, W.A., and Fitzgerald, L.A. 2015. Sand grain size composition influences subsurface
704 oxygen diffusion and distribution of an endemic, psammophilic lizard: Oxygen
705 diffusion in sand limits lizard distribution. *J Zool* 295: 116–121.
706 Ryberg, W.A., and Fitzgerald, L.A. 2016. Landscape composition, not connectivity,
707 determines metacommunity structure across multiple scales. *Ecography* 39: 932–
708 941.
709 Ryberg, W.A., Hill, M.T., Lay, D., and Fitzgerald, L.A. 2012. Observations on the nesting
710 ecology and early life history of the Dunes Sagebrush Lizard (*Sceloporus arenicolus*).
711 *Western North American Naturalist* 72: 582–585.
712 Ryberg, W.A., Hill, M.T., Painter, C.W., and Fitzgerald, L.A. 2013. Landscape pattern
713 determines neighborhood size and structure within a lizard population. *PLoS ONE* 8:
714 e56856.
715 Ryberg, W.A., Hill, M.T., Painter, C.W., and Fitzgerald, L.A. 2014. Linking irreplaceable
716 landforms in a self-organizing landscape to sensitivity of population vital rates for
717 an ecological specialist. *Conservation Biology* 29: 888–898.

718 Schär, S., Eastwood, R., Arnaldi, K.G., Talavera, G., Kaliszewska, Z.A., Boyle, J.H., Espeland, M.,
719 Nash, D.R., Vila, R., and Pierce, N.E. 2018. Ecological specialization is associated with
720 genetic structure in the ant-associated butterfly family Lycaenidae. *Proc. R. Soc. B*
721 285: 20181158.
722 Smolensky, N.L., and Fitzgerald, L.A. 2011. Population variation in dune-dwelling lizards in
723 response to patch size, patch qualtiy and oil and gas development. *The Southwestern*
724 *Naturalist* 56: 315–324.
725 Stephens, M., Smith, N.J., and Donnelly, P. 2001. A new statistical method for haplotype
726 reconstruction from population data. *American Journal Of Human Genetics* 68: 978–
727 989.
728 Swofford, D. 2002. PAUP*, Phylogenetic Analysis Using Parsimony (* and Other Methods).
729 *In* 2nd edition. *Edited By* P. Lemey, M. Salemi, and A.-M. Vandamme. Cambridge
730 University Press, Cambridge.
731 Vandergast, A.G., Bohonak, A.J., Hathaway, S.A., Boys, J., and Fisher, R.N. 2008. Are hotspots
732 of evolutionary potential adequately protected in southern California? *Biological*
733 *Conservation* 141: 1648–1664.
734 Vandergast, A.G., Bohonak, A.J., Weissman, D.B., and Fisher, R.N. 2007. Understanding the
735 genetic effects of recent habitat fragmentation in the context of evolutionary history:
736 phylogeography and landscape genetics of a southern California endemic Jerusalem
737 cricket (Orthoptera: Stenopelmatidae: *Stenopelmatus*). *Molecular Ecology* 16: 977–
738 992.
739 Walkup, D.K., Leavitt, D.J., and Fitzgerald, L.A. 2017. Effects of habitat fragmentation on
740 population structure of dune-dwelling lizards. *Ecosphere* 8: e01729.
741 Walkup, D.K., Ryberg, W.A., Fitzgerald, L.A., and Hibbitts, T.J. 2018. Occupancy and
742 detection of an endemic habitat specialist, the dunes sagebrush lizard (*Sceloporus*
743 *arenicolus*). *Herpetological Conservation and Biology* 13: 497–506.
744 Walkup, D.K., Ryberg, W.A., Fitzgerald, L.A., and Hibbitts, T.J. 2019. From the ground up:
745 microhabitat use within a landscape context frames the spatiotemporal scale of
746 settlement and vacancy dynamics in an endemic habitat specialist. *Landscape Ecol*
747 34: 2631–2647.
748 Wort, E.J.G., Chapman, M.A., Hawkins, S.J., Henshall, L., Pita, A., Rius, M., Williams, S.T., and
749 Fenberg, P.B. 2019. Contrasting genetic structure of sympatric congeneric
750 gastropods: Do differences in habitat preference, abundance and distribution
751 matter? *J Biogeogr* 46: 369–380.
752 Wright, S. 1946. Isolation by distance under diverse systems of mating. *Genetics* 31: 39–59.
753 Young, M.E., Ryberg, W.A., Fitzgerald, L.A., and Hibbitts, T.J. 2018. Fragmentation alters
754 home range and movements of the Dunes Sagebrush Lizard (*Sceloporus arenicolus*).
755 *Can. J. Zool.* 96: 905–912.
756
757

Tables

Table 1. Pairwise F_{ST} values among regions for microsatellite genotypes (above diagonal) and mitochondrial sequence data (below diagonal). Values significantly different from zero (at alpha < 0.05) are indicated in bold. The significance of some values was not able to be determined because of low genetic variability, indicated with italics.

	AA	AB	BA	BB	C	DA	DB	EA	EB	EC
AA		**0.0807**	**0.0349**	*0.0689*	**0.0358**	**0.1443**	**0.1723**	**0.1488**	**0.1654**	**0.1457**
AB	0.0279		0.1077	*0.1911*	0.0749	**0.1988**	0.2374	0.2080	0.2356	0.2010
BA	**0.3389**	**0.3151**		*0.0512*	**0.0264**	**0.1337**	**0.1594**	**0.1349**	**0.1388**	**0.1033**
BB	**0.6593**	**0.7667**	**0.2147**		*0.0807*	*0.1643*	*0.2116*	*0.1688*	*0.1830*	*0.1592*
C	**0.4102**	**0.3688**	**0.4605**	**0.6583**		**0.1271**	**0.1523**	**0.1213**	**0.1350**	**0.1071**
DA	**0.8466**	**0.8584**	**0.8083**	**0.8687**	**0.8503**		**0.0411**	**0.0882**	**0.1188**	**0.0990**
DB	**0.8381**	**0.8395**	**0.7483**	**0.8439**	**0.8173**	**0.3311**		**0.1213**	**0.1554**	0.1302
EA	**0.7984**	**0.7723**	**0.7372**	**0.7842**	**0.7858**	**0.5767**	**0.4206**		**0.1188**	**0.1017**
EB	**0.5554**	**0.4000**	**0.5021**	**0.4513**	**0.5523**	**0.6668**	**0.4663**	**0.5302**		0.0701
EC	**0.8406**	**0.8125**	**0.7540**	**0.8216**	**0.8099**	**0.8872**	**0.8424**	**0.8108**	**0.4119**	

766 **Figure Legends**

767 Figure 1. Collection localities for samples of *S. arenicolus* from New Mexico included in this
768 study and the outline of the species' range and suitable shinnery oak-sand dune habitat
769 (from Laurencio and Fitzgerald, 2010). Specific localities are not shown for Texas due to
770 legal confidentiality agreements with landowners. Colored portions of the species' range
771 correspond to phylogroups and geographic regions referred to in text. Brown indicates
772 potential habitat in Texas where *S. arenicolus* has not been found; one locality exists in this
773 region from 1970. Presence/absence data and habitat suitability maps could be used to
774 more precisely delineate geographic boundaries of the phylogroups within areas of suitable
775 habitat.

776

777 Figure 2. Haplotype networks based on concatenated mtDNA sequences. Circles represent
778 unique haplotypes with the size of the circle corresponding to the relative abundance and
779 the color referring to the region of origin of individuals with that haplotype (see boxes in
780 upper left representing geographic approximations of each region). Lines connecting
781 haplotypes represent one mutational step. Small white circles represent unsampled
782 haplotypes. [Alternate version for individuals with color vision deficiencies included].

783

784 Figure 3. Majority-rules consensus tree from Bayesian phylogenetic analysis of
785 concatenated mtDNA sequence data. Posterior probability for all nodes is 1 unless
786 otherwise indicated. Tips are labeled with a sample name followed by the number of
787 samples with an identical haplotype. Regions of collection are indicated vertically with
788 several exceptions listed parenthetically in terminal name.

789

790 Figure 4. Individual assignment plots from nested Bayesian assignment tests in

791 STRUCTURE. Results at alternate values of K are shown for some subsets of individuals.

792

793 Figure 5. Estimates of divergence and expansion times as well as current and historical

794 effective population sizes for the best supported model from ABC analysis of the complete

795 genetic dataset.

Figure 1

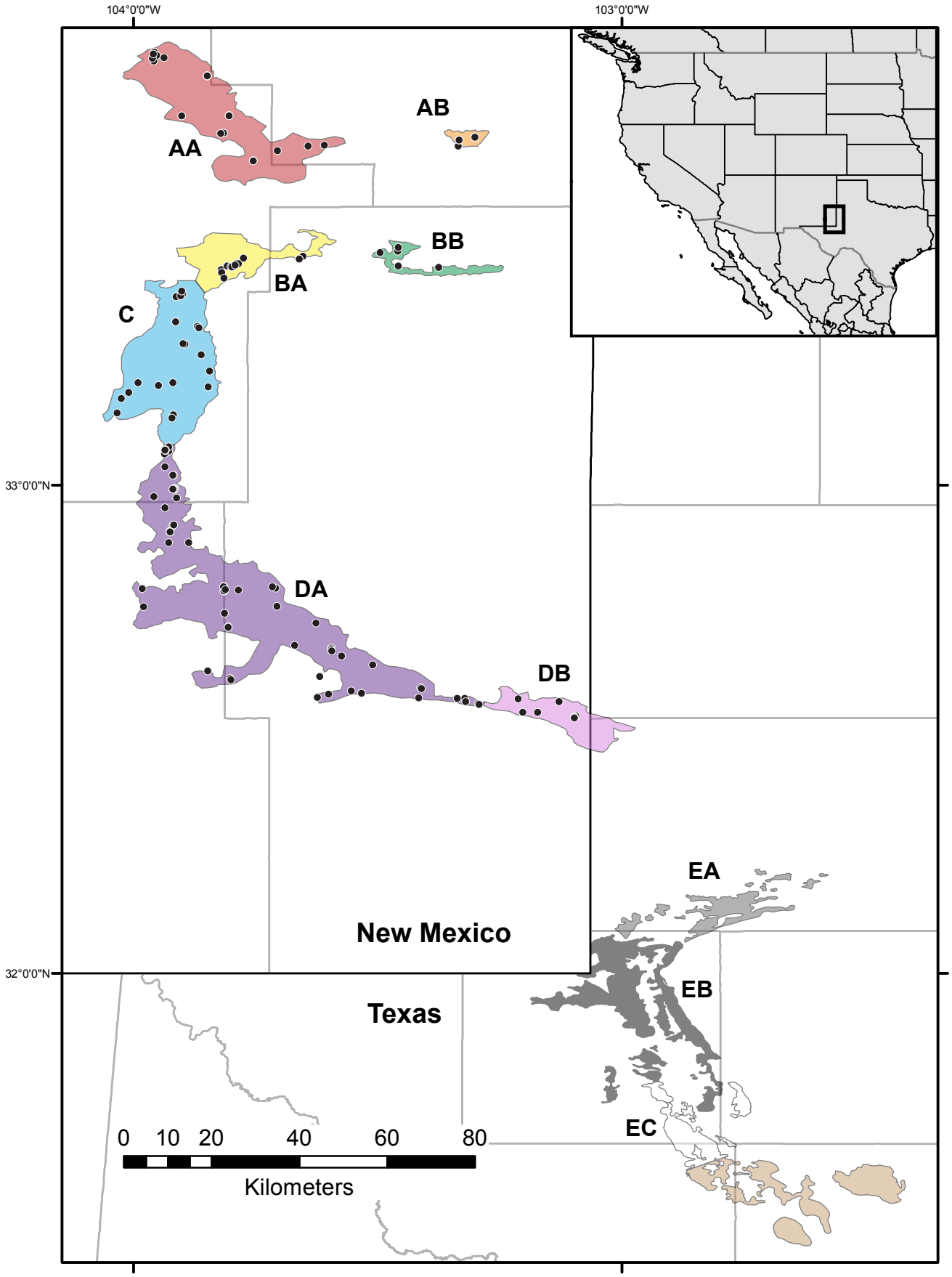

Figure 2

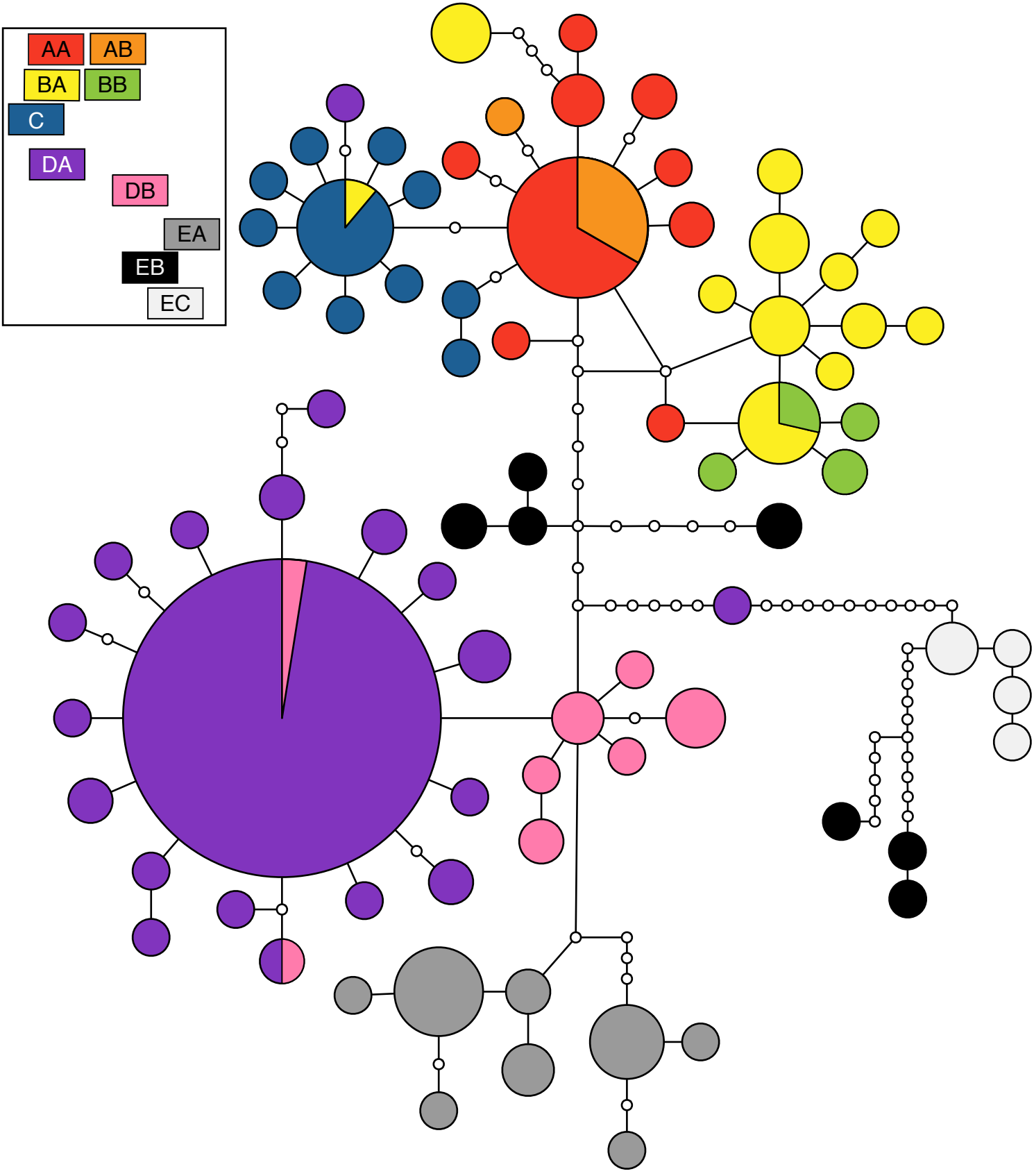

Figure 2 (alternate version)

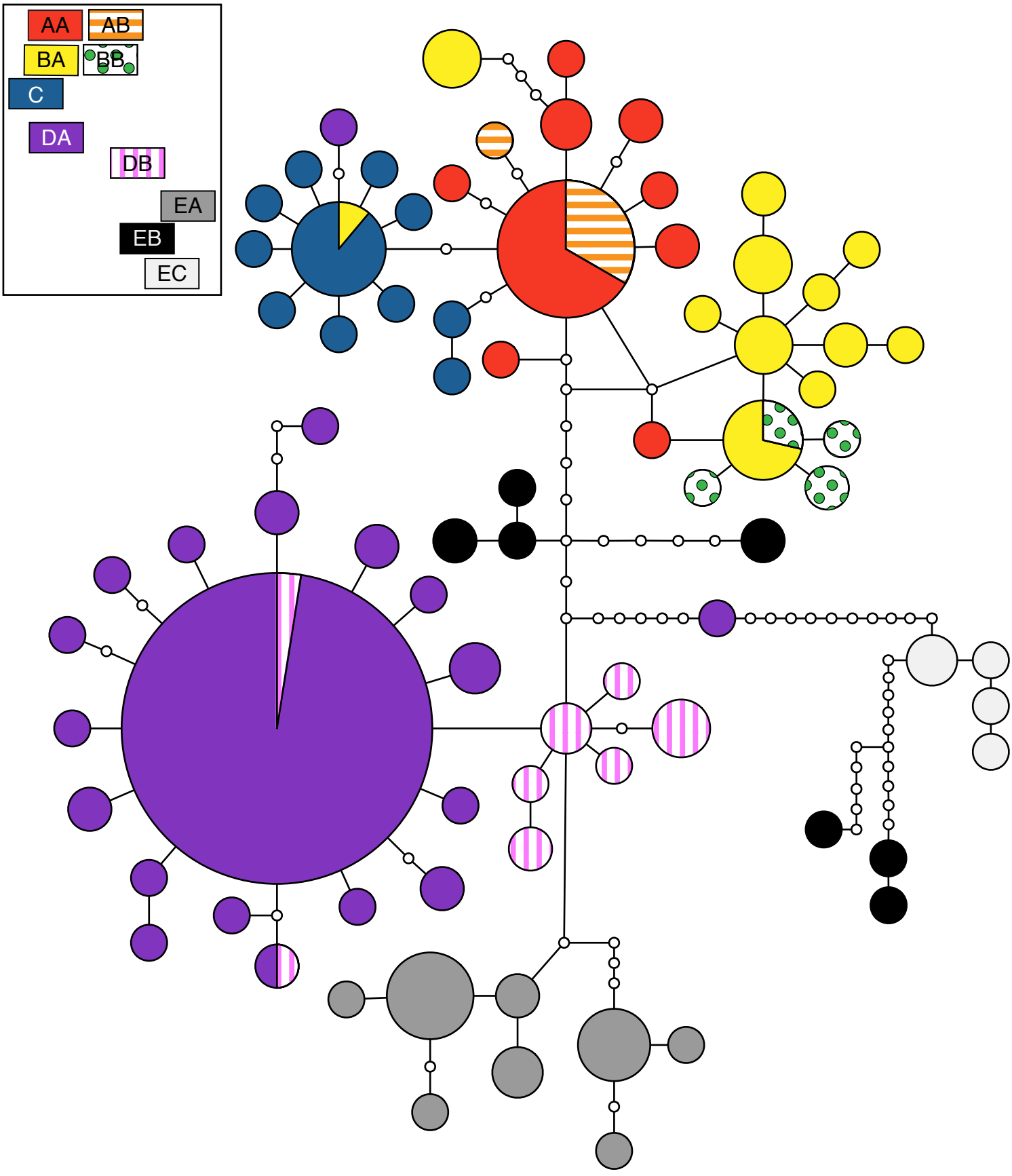

Figure 3

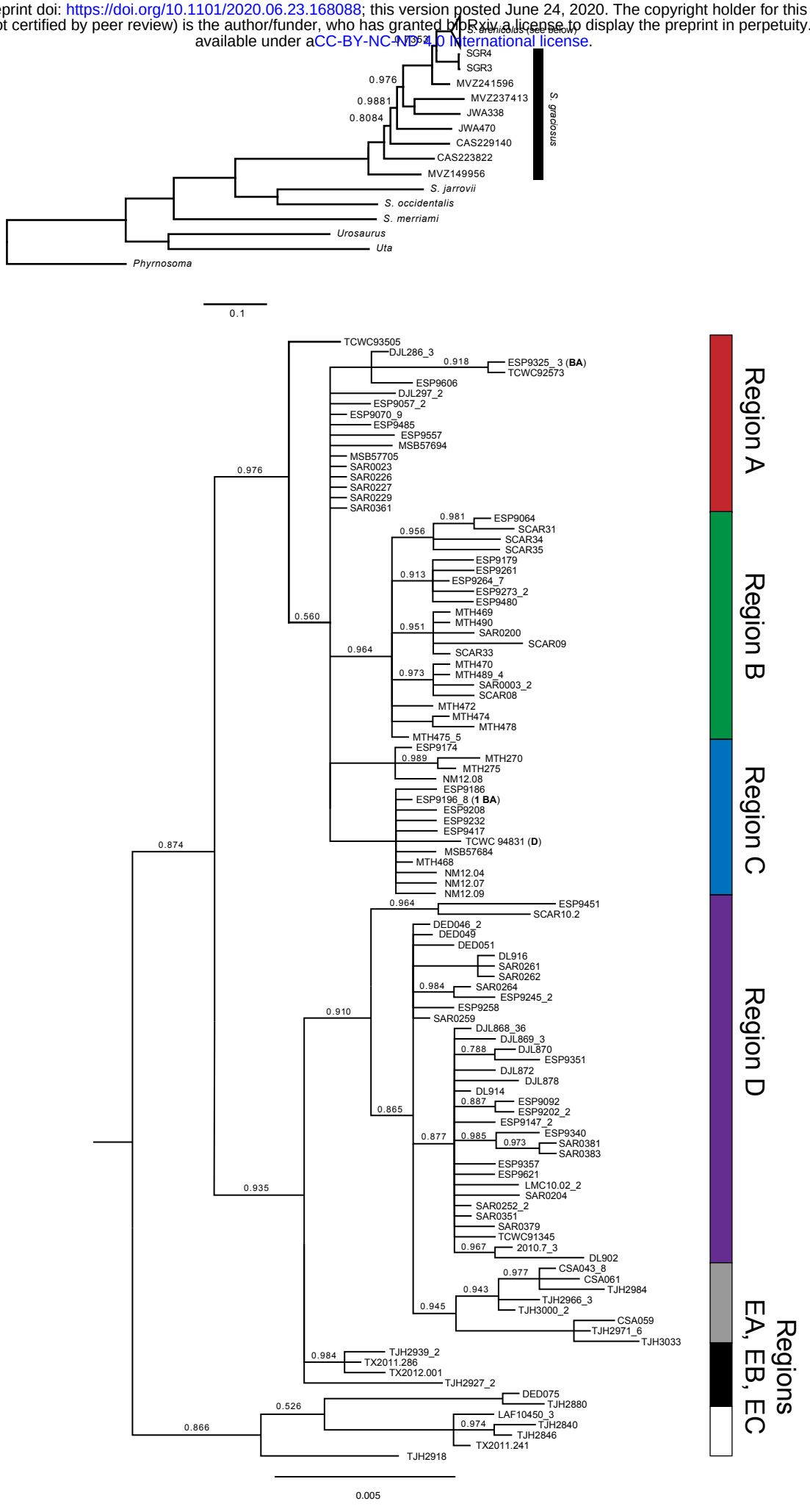

Figure 4

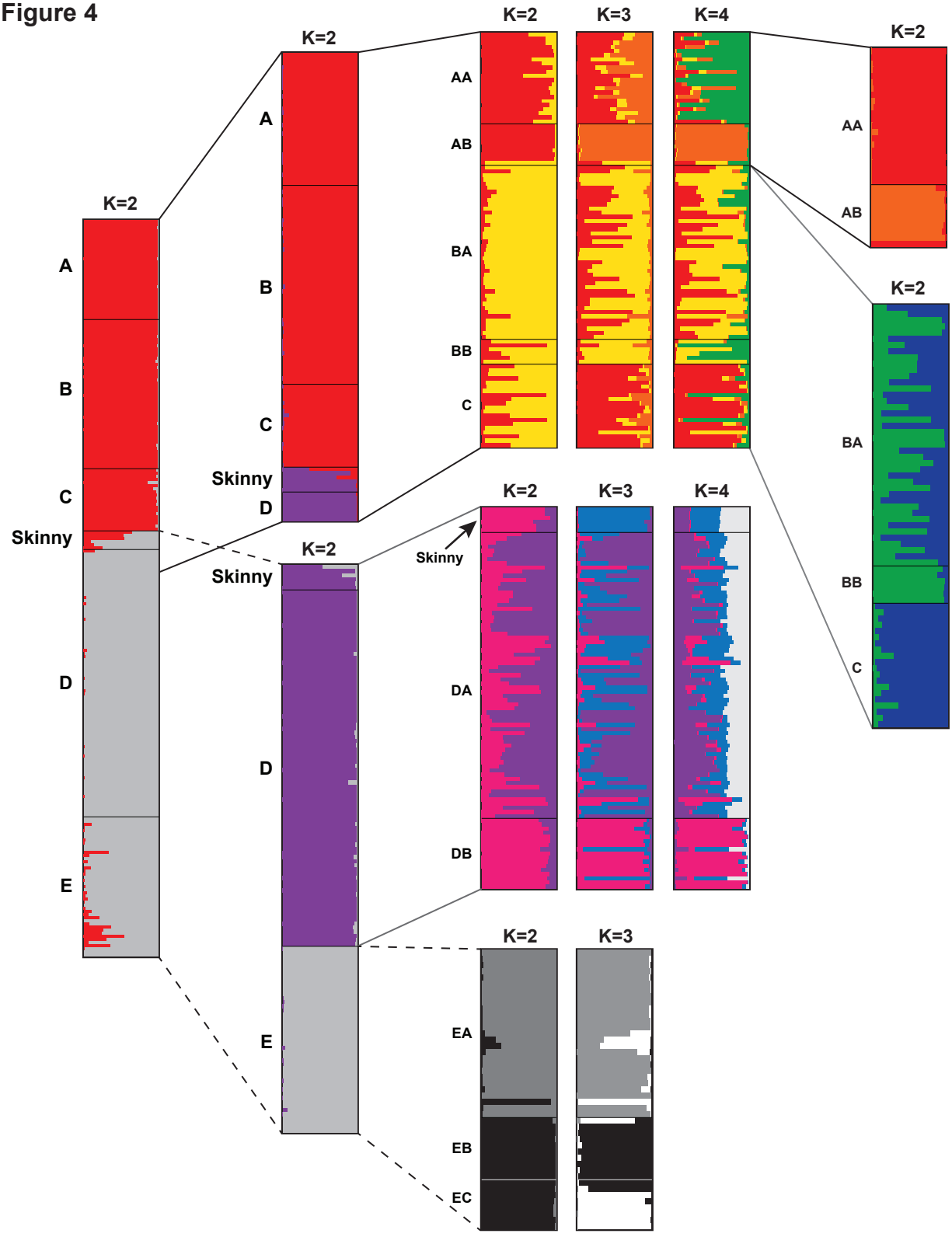

Figure 5